Hsieh, C. H., & Griffith, J. D. (1988) *Cell 52*, 535-544.
Kadesch, T. R., & Chamberlin, M. J. (1982) *J. Biol. Chem. 257*, 5286-5295.
Kao, S. Y., Calman, A. F., Luciw, P. A., & Peterlin, B. M. (1987) *Nature (London) 330*, 489-493.
Kerppola, T. K., & Kane, C. M. (1988) *Mol. Cell. Biol. 8*, 4389-4394.
Kessler, M. M., Beckendorf, R. C., Westhafer, M. A., & Nordstrom, J. L. (1986) *Nucleic Acids Res. 14*, 4939-4952.
Koo, H. S., Wu, H. M., & Crothers, D. M. (1986) *Nature 320*, 501-506.
Lattier, D. L., States, J. C., Hutton, J. J., & Wiginton, D. A. (1989) *Nucleic Acids Res. 17*, 1061-1076.
Lavialle, C., Sekura, R., Madden, M.-J., & Salzman, N. P. (1982) *J. Biol. Chem. 257*, 12458-12466.
Levin, J. R., & Chamberlin, M. J. (1987) *J. Mol. Biol. 196*, 61-84.
Logan, J., Falck-Pedersen, E., Darnell, J. E., & Shenk, T. (1987) *Proc. Natl. Acad. Sci. U.S.A. 84*, 8306-8310.
Maderious, A., & Chen-Kiang, S. (1984) *Proc. Natl. Acad. Sci. U.S.A. 81*, 5931-5935.
Mazabrand, A., Scherly, D., Muller, F., Rungger, D., & Clarkson, S G. (1987) *J. Mol. Biol. 195*, 835-845.
Mok, M., Maderious, A., & Chen-Kiang, S. (1984) *Mol. Cell. Biol. 4*, 2031-2040.
Natori, S. (1982) *Mol. Cell. Biochem. 46*, 173-187.
Nepveu, A., & Marcu, K. B. (1986) *EMBO J. 5*, 2859-2865.
Neuman de Vegvar, H. E., Lund, E., & Dahlberg, J. E. (1986) *Cell 47*, 259-266.
Nevins, J. R., & Wilson, M. C. (1981) *Nature (London) 290*, 113-118.
Okayama, H., & Berg, P. (1983) *Mol. Cell. Biol. 3*, 280-289.
Pfeiffer, P., Hay, N., Pruzan, R., Jakobovits, E. B., & Aloni, Y. (1983) *EMBO J. 2*, 185-191.
Platt, T. (1986) *Annu. Rev. Biochem. 55*, 339-372.
Rappaport, J., Cho, K., Saltzman, A., Prenger, J., Golomb, M., & Weinmann, R. (1988) *Mol. Cell. Biol. 8*, 3136-3142.
Reddy, V. B., Ghosh, P. K., Lebowitz, P., Piatak, M., & Weissman, S. M. (1979) *J. Virol. 30*, 279-296.
Reinberg, D., & Roeder, R. G. (1987) *J. Biol. Chem. 262*, 3331-3337.
Reines, D., Wells, D., Chamberlin, M. J., & Kane, C. M. (1987) *J. Mol. Biol. 196*, 299-312.
Reines, D., Chamberlin, M. J., & Kane, C. M. (1989) *J. Biol. Chem. 264*, 10799-10809.
Resnekov, O., & Aloni, Y. (1989) *Proc. Natl. Acad. Sci. U.S.A. 86*, 12-16.
Salser, W. (1977) *Cold Spring Harbor Symp. Quant. Biol. 42*, 985-1002.
Skarnes, W. C., Tessier, D. C., & Acheson, N. H. (1988) *J. Mol. Biol. 203*, 153-171.
Sollner-Webb, B., & Tower, J. (1986) *Annu. Rev. Biochem. 55*, 801-830.
Sopta, M., Carthew, R. W., & Greenblatt, J. (1985) *J. Biol. Chem. 260*, 10353-10360.
Tabor, S., & Richardson, C. C. (1987) *Proc. Natl. Acad. Sci. U.S.A. 84*, 4767-4771.
Telesnitsky, A., & Chamberlin, M. (1989) *Biochemistry 28*, 5210-5218.
Thayer, G. C., & Brosius, J. (1985) *Mol. Gen. Genet. 199*, 55-58.
Ulanovsky, L. E., & Trifonov, E. N. (1987) *Nature 326*, 720-722.
Whitelaw, E., & Proudfoot, N. (1986) *EMBO J. 5*, 2915-2922.
Wright, S., & Bishop, J. M. (1989) *Proc. Natl. Acad. Sci. U.S.A. 86*, 505-509.
Wu, H. M., & Crothers, D. M. (1984) *Nature 308*, 509-513.
Yanisch-Perron, C., Vieira, J., & Messing, J. (1985) *Gene 33*, 103-119.
Zuker, M., & Stiegler, P. (1981) *Nucleic Acids Res. 9*, 133-148.

Thermodynamic and Spectroscopic Study of Bulge Loops in Oligoribonucleotides†

Carl E. Longfellow,‡ Ryszard Kierzek,§ and Douglas H. Turner*,‡

Department of Chemistry, University of Rochester, Rochester, New York 14627, and Institute of Bioorganic Chemistry, Polish Academy of Sciences, 60-704 Poznan, Noskowskiego 12/14, Poland

Received January 6, 1989; Revised Manuscript Received June 1, 1989

ABSTRACT: Thermodynamic parameters for bulge loops of one to three nucleotides in oligoribonucleotide duplexes have been measured by optical melting. The results indicate bulges B_n of A_n and U_n have similar stabilities in the duplexes, GCG^{B_n}GCG + CGCCGC. The stability increment for a bulge depends on more than its adjacent base pairs. For example, the stability increment for a bulge is affected more than 1 kcal/mol by changing two nonadjacent base pairs or by adding terminal unpaired nucleotides (dangling ends) three base pairs away. Thus a nearest-neighbor approximation for helixes with bulges is oversimplified. Many of the non-self-complementary strands used in this study were observed to form homoduplexes. Such duplexes with GA mismatches were particularly stable.

A bulge loop forms in double-helical RNA when the helix is interrupted by unpaired nucleotides on only one strand. Such structures are known to be important for binding of coat protein to R17 virus (Romaniuk et al., 1987) and of ribosomal protein L18 to ribosomal RNA (Peattie et al., 1981; Christiansen et al., 1985). Bulge loops are also thought to be important for intron splicing (Parker et al., 1987; Schmelzer & Schweyen, 1987) and for feedback regulation of the L10 operon in *Escherichia coli* (Climie & Friesen, 1987). Although their functional significance is often unknown, bulge loops are widespread in accepted secondary structures of many

† This work was supported by National Institutes of Health Grant GM22939.
‡ University of Rochester.
§ Polish Academy of Sciences.

0006-2960/90/0429-278$02.50/0

RNAs (Gutell et al., 1985, 1988; Erdmann & Wolters, 1986; Michel & Dujon, 1983; Michel & Jacquier, 1988). Despite this ubiquity, relatively little is known about thermodynamic parameters for bulges. Measurements have been made on bulges of one nucleotide embedded in poly(A)·poly(U) (Fink & Crothers, 1972; Fink & Krakauer, 1975), in hairpin stems (Groebe & Uhlenbeck, 1989), and in deoxyoligonucleotides (Woodson & Crothers, 1987). A bulge of five nucleotides has been studied in the colicin fragment of 16S rRNA (Yuan et al., 1979). This lack of data is a concern because thermodynamic parameters for bulges are important for predicting RNA secondary structure from sequence (Tinoco et al., 1973; Papanicolaou et al., 1984; Zuker & Stiegler, 1981; Turner et al., 1988; Zuker, 1989). This paper reports thermodynamic parameters for bulge loops of one to three nucleotides in oligoribonucleotides of various sequence. The results indicate the effects of bulges on helix stability are more complex than suggested by current approximations.

Materials and Methods

Synthesis and Purification of RNA. Oligomers were synthesized on solid support by phosphoramidite chemistry (Kierzek et al., 1986). After deblocking with ammonia, oligomers were purified with high-performance liquid chromatography (HPLC) on a Hamilton PRP-1, 150 mm × 4.1 mm column (Ikuta et al., 1984). A gradient was run from 100% buffer A (aqueous 0.01 M ammonium acetate, pH 6.8) to 70% buffer B (50% v/v acetonitrile and aqueous 0.01 M ammonium acetate, pH 6.8). The total time for the gradient was 35 min with a flow rate of 2 mL/min. The partially blocked oligomers eluted at about 30% acetonitrile. They were dried down and deblocked further with acid (Kierzek et al., 1986). After the acid treatment, oligomers were further purified and desalted with a C-18 Sep-Pak cartridge (Freier et al., 1985).

Purity was checked by HPLC on a Beckman C-8, 150 mm × 4.6 mm column. The gradient was run from 100% buffer A (aqueous 0.01 M sodium phosphate, pH 7) to 60% buffer B (50% v/v methanol and aqueous 0.01 M sodium phoshate, pH 7). The total time for the gradient was 60 min with a flow rate of 1 mL/min. Final purity of the oligomers was greater than 95%.

A further check of sequence and purity was made by measuring NMR[1] spectra of the nonexchangeable protons at 70 °C. Chemical shifts were compared with those predicted from a nearest-neighbor model (Hader et al. 1985). Spectra and measured and predicted chemical shifts are shown in the supplementary material (see paragraph at end of paper regarding supplementary material). The average and maximum deviations between predicted and measured chemical shifts are 0.014 and 0.044 ppm, respectively.

Melting Curves. Oligomers were dissolved in 1 M NaCl, 10 mM sodium cacodylate, 0.5 mM ethylenediaminetetraacetic acid (EDTA), pH 7 buffer. Strand concentrations were determined at 280 nm with the high-temperature absorption. Extinction coefficients were calculated as described previously (Freier et al., 1983; Richards, 1975) and are listed in Tables I and II and in the supplementary material. Optical melting curves were measured on a Gilford 250 spectrophotometer with a thermoprogrammer (Petersheim & Turner, 1983). Samples were heated to 90 °C for 5 min immediately prior to starting melts. Typical curves are shown in the supplementary material.

[1] Abbreviations: CD, circular dichroism; EDTA, ethylenediaminetetraacetic acid; NMR, nuclear magnetic resonance.

Data Analysis. Melting curves of single strands were fit with the one-dimensional Ising model (Applequist, 1963; Zimm & Bragg, 1959; Dewey & Turner, 1982). A nonlinear least-squares program fit the data to

$$K_{eq} = \exp\frac{-\Delta H^\circ + T\Delta S^\circ}{RT} \quad (1)$$

$$\alpha = 0.5 + 0.5(K_{eq} - 1)/[(1 - K_{eq})^2 + 4\sigma K_{eq}]^{1/2} \quad (2)$$

$$A(T) = (1 - \alpha)A_{rc} + \alpha A_{st} \quad (3)$$

where K_{eq} is the equilibrium constant for random coils going to stacked strands, α is the fraction of stacked single strands, $1 - \alpha$ is the fraction of random coils, $A(T)$ is the absorbance at temperature T, A_{rc} is the absorbance when all strands are random coil, A_{st} is the absorbance when all strands are stacked, and σ is the cooperativity of the melting transition. σ was fixed at either 1 or 0.5, and the data were fit with the parameters ΔH°, ΔS°, A_{rc}, and A_{st}.

Melting curves of homoduplexes were fit with the nonlinear least-squares program described by Petersheim and Turner (1983) and Freier et al. (1983). This program was also revised to fit melting curves of non-self-complementary duplexes. In this case, the extinction coefficient, ϵ, and the absorbance, $A(T)$, of the solution at any temperature are given by

$$\epsilon(T) = A(T)/LC_T = \epsilon_{ds}\alpha' + 0.5\epsilon_{ss1}(1 - \alpha') + 0.5\epsilon_{ss2}(1 - \alpha') \quad (4)$$

Where α' is the fraction of double-stranded RNA, L is the pathlength of the cell, C_T is the total strand concentration, and ϵ_{ds}, ϵ_{ss1}, and ϵ_{ss2} are extinction coefficients for the double strand and the two single strands, respectively. This equation can be simplified by noting that the concentrations of the single strands are equal and by averaging the single-strand extinction coefficients to give $\epsilon_{ss} = (\epsilon_{ss1} + \epsilon_{ss2})/2$:

$$\epsilon(T) = A(T)/LC_T = \epsilon_{ds}\alpha' + \epsilon_{ss}(1 - \alpha') \quad (5)$$

ϵ_{ds} and ϵ_{ss} are assumed to be linear functions of temperature:

$$\epsilon_{ds}(T) = m_{ds}T + b_{ds} \quad (6a)$$

$$\epsilon_{ss}(T) = m_{ss}T + b_{ss} \quad (6b)$$

The equilibrium constant for this system can be described in terms of α' as

$$K_{eq}' = 2\alpha'/[C_T(1 - \alpha')^2] = \exp\frac{-\Delta H^\circ + T\Delta S^\circ}{RT} \quad (7)$$

The program fits absorbance vs temperature data with the parameters ΔH°, ΔS°, m_{ds}, b_{ds}, m_{ss}, and b_{ss}.

Two methods were used to obtain thermodynamic parameters for duplexes. The first is to average the fitted ΔH°'s and ΔS°'s. The second method is to plot T_M^{-1} vs log $(C_T/4)$ to obtain ΔH° and ΔS° (Borer et al., 1974):

$$T_M^{-1} = \frac{2.3R}{\Delta H^\circ}\log\left(\frac{C_T}{4}\right) + \frac{\Delta S^\circ}{\Delta H^\circ} \quad (8)$$

The melting curves for GCGGCG + CGCCGC, GCGUGCG + CGCCGC, GCGUUGCG + CGCCGC, GCGUUUGCG + CGCCGC, GCGAAAGCG + CGCCGC, GCGGCG + CGCAACGC, and GCGGCG + CGCAAACGC were also fit by replacing the linear approximation of ϵ_{ss} with the temperature dependence of ϵ_{ss} as measured directly with the single strands. For these fits, C_T was a variable parameter because the high temperature absorbance is well-defined by the single-strand melts.

Calculation of Species in Solution. The fraction of each species in a solution of two strands, A and B, was calculated by assuming that the total concentrations of each strand are

Table I: Thermodynamic Parameters for Homoduplex Formation in 1 M NaCl[a]

oligomer	ϵ(280 nm) × 10^{-3}	$-\Delta H°$ (kcal/mol)	$-\Delta S°$ (eu)	$-\Delta G°_{37}$ (kcal/mol)	T_M (°C) 10^{-4} M	T_M (°C) 5 × 10^{-5} M	$-\Delta G°_{37}$(pred) (kcal/mol)
CGCCGC	2.94	24.0	67.7	3.0	5.9	1.5	2.8
CGCACGC	3.21	33.7	98.9	3.0	14.4	11.0	1.9
GCGAGCG	3.61	55.5 (65.6)	158 (190)	6.6 (6.6)	42.1	39.2	4.7
GCGAAGCG	3.96	41.5 (48.0)	115 (137)	5.8 (5.5)	38.2	35.0	3.9
CGCCGCA	3.11	39.5	113	4.5	27.7	24.5	6.2
CGCACGCA	3.38	28.3	79.3	3.7	16.8	12.8	5.3
GCGGCGA	3.51	51.2	144	6.5	41.9	39.7	5.6
GCGAGCGA	3.82	57.5 (66.8)	162 (192)	7.3 (7.4)	45.8	43.3	4.7
GCGAAGCGA	4.17	32.3	85.5	5.8	38.1	33.9	3.9
GACCGCA	3.16	27.7	78.0	3.5	14.5	10.4	3.6
GCGAGUCA	3.63	27.6	76.1	4.0	18.9	15.0	3.0
CGUAUGCU	3.29	30.1	84.7	3.9	19.6	15.2	3.9
GCAACGA	3.01	31.7	93.6	2.7	10.1	6.7	3.0

[a] Parameters not in parentheses were derived by averaging parameters from fits of melting curves to the self-complementary duplex model. Parameters in parentheses were derived from T_M^{-1} vs log C_T plots. Parameters for sequences with T_M's below 25 °C should be considered as only rough approximations. Errors in $\Delta H°$'s and $\Delta S°$'s for other sequences with and without T_M^{-1} plots are estimated as ±10 and ±20%, respectively.

equal and that one strand can form both a homo- and a heteroduplex:

$$A + A \rightleftarrows A_2 \qquad K_1 = [A_2]/[A]^2 \qquad (9a)$$

$$A + B \rightleftarrows AB \qquad K_2 = [AB]/[A][B] \qquad (9b)$$

The total concentrations of A and B are known, and the two equilibrium constants can be calculated from measured thermodynamic parameters. Solving for the concentration of A gives a cubic equation: $-2K_2K_1[A]^3 - (2K_1 + K_2)[A]^2 - [A] + C_T/2 = 0$. The concentration of A was solved for with Newton's method (Swokowski, 1983). The concentrations of the other species are simply $[A_2] = K_1[A]^2$, $[B] = 2[A_2] + [A]$, and $[AB] = K_2[A][B]$. These concentrations can then be converted to fractions of total strands.

Spectroscopy. Nuclear magnetic resonance (NMR) spectra were measured on a 500-MHz Varian VXR-500S spectrometer. Circular dichroism (CD) spectra were measured on a Jasco J-40 spectropolarimeter.

Results

Single-Strand Melting. The strands used in this work are not self-complementary if only Watson–Crick pairing is allowed. To test for self-complementary interactions, each strand was melted separately. Several strands had broad transitions with small hypochromicities. This is indicative of weak single-strand stacking. Many of the strands, however, have sharper transitions with considerable hypochromicity. These strands were melted at two or more concentrations differing by at least a factor of 9. In many cases, the melting behavior was independent of concentration, indicating a unimolecular process, probably single-strand stacking. These melting curves were fit to the unimolecular model described under Materials and Methods (Applequist, 1963; Zimm & Bragg, 1959; Dewey & Turner, 1979). The thermodynamic parameters derived by assuming a cooperativity parameter σ of 1 or 0.5 are listed in the supplementary material.

Previous optical studies of the thermodynamics of single-strand melting in poly(riboadenylic acid) and poly(ribocytidylic acid) have resulted in values of $\Delta H°$ ranging from −8 to −13 kcal/mol, assuming $\sigma = 1$ (Dewey & Turner, 1979; Freier et al., 1981; Leng & Felsenfeld, 1966; Applequist & Damle, 1966; Stannard & Felsenfeld, 1975; Brahms et al., 1967). Most of the values reported here for concentration-independent single strands are similar to those for the polymers. The $\Delta H°$ values for GCGGCG and GCGAAGUCA are −21.2 and −23.6 kcal/mol, however, suggesting some single-strand sequences may have special properties. Alternatively, GCGGCG and GCGAAGUCA may aggregate. This could result in melting behavior that is apparently concentration independent. For example, the T_M for GCGGCG was concentration independent from 2×10^{-4} to 5×10^{-6} M. When the concentration reached 3×10^{-6} M, the T_M dropped by 6 °C. This is expected for aggregation.

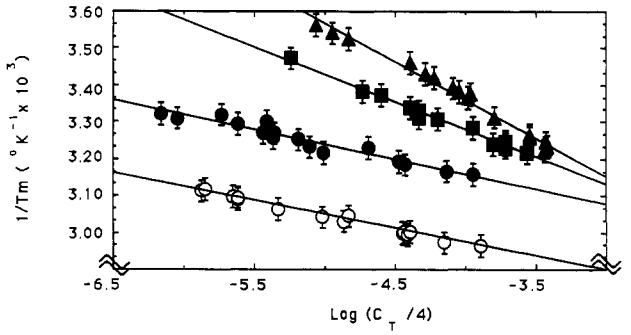

FIGURE 1: Reciprocal melting temperature vs log (concentration/4) plots for GCGGCG + CGCCGC (○), GCGAGCG + CGCCGC (●), GCGAAGCG + CGCCGC (■), and GCGAAAGCG + CGCCGC (▲) in 1 M NaCl, 0.01 M sodium cacodylate, and 0.5 mM EDTA, pH 7.

Surprisingly, many of the non-self-complementary strands have concentration-dependent melting curves, indicating homoduplex formation. For these sequences, melting curves were fit with the self-complementary duplex model described by Petersheim and Turner (1983). Thermodynamic parameters derived from these fits are listed in Table I. GCGAGCG, GCGAAGCG, and GCGAGCGA were melted at several concentrations, and plots of T_M^{-1} vs log C_T are shown in the supplementary material. Thermodynamic parameters from these plots are listed in parentheses in Table I.

Double-Strand Melting. Appropriate pairs of single strands were mixed in equimolar proportions to give duplexes with or without bulged nucleotides. All these combinations had concentration-dependent melting curves. The melting curves were fit with the non-self-complementary, two-state model described under Materials and Methods. Typical plots of T_M^{-1} vs log $C_T/4$ are shown in Figure 1 and in the supplementary material. The thermodynamic parameters derived from these plots and from fits of the melting curves are listed in Table II. Also listed in Table II are thermodynamic parameters predicted from the nearest-neighbor model for the four duplexes without bulges (Freier et al., 1986; Turner et al., 1988). The maximum differences between predicted and measured $\Delta G°_{37}$'s and $\Delta H°$'s are 10 and 18%, respectively; the average differences are 4 and 12%, respectively. This is similar to the

Table II: Thermodynamic Parameters of Duplex Formation in 1 M NaCl for Non-Self-Complementary Duplexes[a]

		T_M^{-1} vs log (C_T/4)				av from fits			
oligomer	ϵ(280 nm) × 10^{-3}	$-\Delta H°$ (kcal/mol)	$-\Delta S°$ (eu)	$-\Delta G°_{37}$ (kcal/mol)	T_M (°C) at 10^{-4} M	$-\Delta H°$ (kcal/mol)	$-\Delta S°$ (eu)	$-\Delta G°_{37}$ (kcal/mol)	T_M (°C) at 10^{-4} M
GCGGCG + CGCCGC	31.2	58.5 (56.6)	155 (149)	10.4 (10.3)	58.7 (59.5)	57.9	153	10.4	59.0
GCGAGCG + CGCCGC	32.8	57.0	162	6.9	38.8	46.8	129	6.9	39.6
GCGUGCG + CGCCGC	31.9	55.2	157	6.7	38.0	40.5	108	6.9	40.2
GCGGCG + CGCACGC	32.6	66.4	192	6.9	38.7	45.8	126	6.8	38.9
GCGAAGCG + CGCCGC	34.5	30.7	82.3	5.2	23.7	32.4	87.5	5.2	25.0
GCGUUGCG + CGCCGC	33.5	28.3	75.1	5.0	21.3	26.5	68.6	5.2	22.7
GCGGCG + CGCAACGC	34.3	47.2	135	5.4	30.0	24.5	59.0	6.2	32.5
GCGAAAGCG + CGCCGC	36.3	22.1	55.9	4.7	13.8	30.8	85.1	4.4	16.9
GCGUUUGCG + CGCCGC	35.1	22.0	55.3	4.8	14.9	27.9	74.6	4.7	18.1
GCGGCG + CGCAAACGC	36.1	63.7	184	6.7	38.0	49.3	137	6.7	38.1
GCGGCGA + CGCCGCA	33.1	84.1 (73.0)	224 (193)	14.6 (13.1)	69.7 (68.7)	77.6	205	14.0	70.0
GCGAGCGA + CGCCGCA	34.6	84.5	242	9.5	48.2	54.6	148	8.6	49.4
GCGGCGA + CGCACGCA	34.4	69.0	195	8.7	46.9	55.1	150	8.5	48.3
GCGAAGCGA + CGCCGCA	36.4	54.4	154	6.7	38.2	35.2	91.6	6.8	39.5
GCGGCGA + CGCAACGCA	36.2	78.8	231	7.1	39.1	47.4	130	7.0	39.8
GCGAAAGCGA + CGCCGCA	38.1	23.6	58.7	5.4	22.2	24.1	60.6	5.3	22.1
GCGGCGA + CGCAAACGCA	37.9	75.3	219	7.3	40.1	46.7	127	7.3	41.9
GCAACGA + CGUUGCU	30.1	78.8 (64.4)	224 (178)	9.2 (9.1)	47.9 (50.5)	62.8	174	8.9	48.9
GCAACGA + CGUAUGCU	31.5	50.3	147	4.6	25.5	43.2	123	5.0	26.6
GACCGCA + GCGGUCA	32.4	68.0 (76.1)	180 (203)	12.1 (12.7)	64.8 (66.0)	47.6	119	10.7	66.4
GACCGCA + GCGAGUCA	33.9	97.6	282	10.1	48.9	70.9	199	9.3	49.5
GACCGCA + GCGAAGUCA	35.7	49.4	138	6.6	37.5	40.9	110	6.8	39.0
GACCGCA + GCGAAAGUCA	37.4	82.3	249	5.0	31.5	32.3	83.7	6.3	34.8

[a] Errors in $\Delta H°$ and $\Delta S°$ are estimated as ±10%. Additional significant figures are given to allow accurate calculation of T_M. Parameters in parentheses are predictions based on parameters of Freier et al. (1986).

Table III: Thermodynamic Parameters for Duplex Formation with Measured Temperature Dependence of Single-Strand Extinction[a]

	T_M^{-1} vs log (C_T/4)				av from fits			
oligomer	$-\Delta H°$ (kcal/mol)	$-\Delta S°$ (eu)	$-\Delta G°_{37}$ (kcal/mol)	T_M (°C) at 10^{-4} M	$-\Delta H°$ (kcal/mol)	$-\Delta S°$ (eu)	$-\Delta G°_{37}$ (kcal/mol)	T_M (°C) at 10^{-4} M
GCGGCG + CGCCGC	49.1 (58.5)	127 (155)	9.8 (10.4)	58.5 (58.7)	55.9 (57.9)	148 (153)	10.0 (10.4)	57.5 (59.0)
GCGUGCG + CGCCGC	46.7 (55.3)	131 (157)	6.1 (6.7)	34.0 (38.0)	50.4 (40.6)	144 (108)	5.8 (6.9)	32.2 (40.2)
GCGUUGCG + CGCCGC	33.3 (28.3)	92.9 (75.1)	4.5 (5.0)	19.1 (21.3)	17.8 (26.5)	40.6 (70.5)	5.2 (5.3)	15.5 (22.7)
GCGGCG + CGCAACGC	16.8 (47.2)	37.7 (157)	5.1 (5.4)	12.8 (30.0)	16.2 (24.5)	35.8 (60.2)	5.1 (6.2)	11.8 (32.5)
GCGAAAGCG + CGCCGC	31.7 (22.1)	88.3 (55.9)	4.3 (4.7)	16.7 (13.8)	16.3 (30.8)	37.4 (85.1)	4.7 (4.4)	5.7 (16.9)
GCGUUUGCG + CGCCGC	29.4 (22.0)	80.2 (55.3)	4.5 (4.8)	17.2 (14.9)	31.9 (27.9)	88.2 (74.6)	4.5 (4.7)	18.8 (18.1)
GCGGCG + CGCAAACGC	38.8 (63.7)	105 (184)	6.2 (6.7)	34.7 (38.0)	29.8 (49.3)	76.2 (137)	6.2 (6.7)	33.3 (38.1)

[a] Errors in $\Delta H°$ and $\Delta S°$ are estimated as ±10%. Additional significant figures are given to allow accurate calculation of T_M. For GCGGCG, the measured $\epsilon(T)$ at 3 × 10^{-6} M strands was used. The thermodynamic parameters that fit the GCGGCG single-strand melt were $\Delta H°$ = −16.5 kcal/mol and $\Delta S°$ = −55.4 eu for σ = 0.5. Parameters in parentheses are from Table II and are provided for easy comparison.

performance previously reported for the nearest-neighbor model (Freier et al., 1986; Kierzek et al., 1986).

The model used to fit the optical melting curves has several assumptions. One assumption is that extinction coefficients for the duplex and single strands are linear functions of temperature. These duplexes are not self-complementary, so potentially this assumption can be avoided. In principle, the measured temperature dependence of single-strand extinction coefficients can be used in the fitting procedure. As discussed above, however, some of the single strands have concentration-dependent melting curves indicating intermolecular associations. For these sequences, determination of the temperature dependence of the true single strands is difficult. Moreover, a major application of thermodynamic parameters derived from this study is to predict RNA structure from sequence. For this application, the parameters will be combined with many parameters determined from self-complementary oligonucleotides (Freier et al., 1986; Turner et al., 1988). Analysis for these oligomers necessarily requires the linear approximation for extinction coefficients. Thus, for uniformity, the same model was used for duplexes listed in Table II. To check the effect of this assumption, melting curves for several duplexes in the GCGGCG + CGCCGC series were analyzed by including the measured temperature-dependent extinction coefficients for single strands. The results are listed in Table III. This correction can have considerable effects on $\Delta H°$ and $\Delta S°$. The average change in $\Delta G°_{37}$, however, is less than 10%. Evidently, errors in $\Delta H°$ and $\Delta S°$ compensate.

Another assumption in the model is that the transition is two state. That is, the molecules are either duplexes or single strands, and there are no partially paired states. If true, then $\Delta H°$ derived from fits of melting curves and from T_M^{-1} vs log (C_T/4) plots should be the same. In practice, agreement within 15% is usually considered sufficient (Freier et al., 1986). Of 23 duplexes listed in Table II, only 6 meet this criterion. This suggests most of the transitions are not two state or that the nonlinear extinctions of single strands differentially affect the two methods for determining $\Delta H°$. The results in Table III support this suggestion. Three sequences that are non two state with linear base lines become two state when experimental single-strand absorbances are included. Not all sequences become two state, however. Clearly, most of the $\Delta H°$'s and $\Delta S°$'s must be viewed with caution. Empirical evidence, however, suggests that even when a transition is not two state, $\Delta G°$'s obtained from optical studies are reliable near the melting temperature (Freier et al., 1984). A measure of the potential error introduced by the model is the difference in

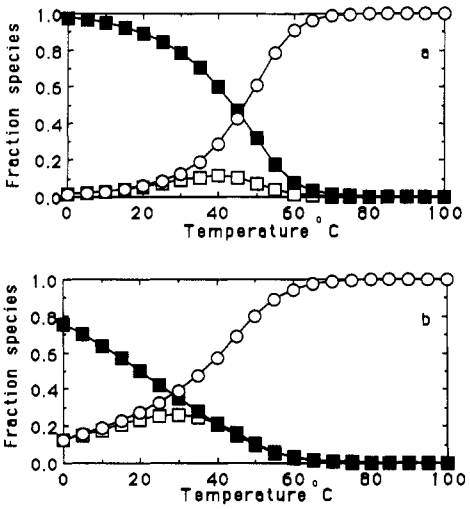

FIGURE 2: At a total strand concentration of 5×10^{-4} M, the calculated fraction of various species vs temperature. (a) GCGAGCG + CGCCGC: $(GCGAGCG)_2$ (□), GCGAGCG + CGCCGC (■), and single strands (○). (b) GCGAAGCG + CGCCGC: $(GCGAAGCG)_2$ (□), GCGAAGCG + CGCCGC (■), and single strands. (○).

$\Delta G°$ obtained from fits and from T_M^{-1} vs log $(C_T/4)$ plots. Inspection of Table II indicates this error is less than 10% in most cases and averages 5%, even when $\Delta G°$'s are extrapolated to 37 °C. Again, errors in $\Delta H°$ and $\Delta S°$ compensate.

As described above, concentration-dependent melting curves were observed for several of the single strands in this study. In many cases, the T_M for these homoduplexes was similar to or higher than the T_M for the heteroduplex containing a bulge. Thus interpretation of thermodynamic parameters requires knowledge of the distribution of species in solution. For example, if both homo- and heteroduplexes are present, then melting curves only provide some limits on thermodynamic parameters. Figure 2 illustrates this for the combinations of CGCCGC with GCGAGCG and GCGAAGCG. For the log C_T thermodynamic parameters given in Tables I and II, the results of a multiple equilibrium calculation of the fraction of total strands in each species is shown for a total strand concentration of 5×10^{-4} M. For CGCCGC + GCGAGCG, the fraction of strands as $(GCGAGCG)_2$ is always less than 12%. This is true, even though the T_M's for CGCCGC + GCGAGCG and $(GCGAGCG)_2$ are 39 and 42 °C, respectively, at 10^{-4} M strands. Evidently, CGCCGC pulls the equilibrium to the bulged duplex. The situation is less clear for CGCCGC + GCGAAGCG. Here the T_M of the bulged duplex is more than 10 °C lower than that of $(GCGAAGCG)_2$. As shown in Figure 2, the fraction of strands as $(GCGAAGCG)_2$ may rise as high as 26%. To check these conclusions, CD and NMR spectroscopies were used to look for the presence of homoduplexes in selected mixtures.

CD Spectra. Figure 3 presents CD spectra for the individual strands CGCCGC, GCGAGCG, and GCGAAGCG and for the equimolar combinations of CGCCGC with GCGGCG, GCGAGCG, and GCGAAGCG. Figure 4 presents CD spectra for the individual strands GCGGCGA and CGCAACGCA and for the equimolar combinations of GCGGCGA with CGCCGCA, CGCACGCA, and CGCAACGCA. All the strand combinations have CD spectra characteristic of A-form helixes (Tunis-Schneider & Maestre, 1970). The negative peak at 295 nm observed for the perfectly matched duplexes, however, is either missing or much reduced for the bulged duplexes. Moreover, with the exception of CGCACGCA + GCGGCGA, the large, positive band around

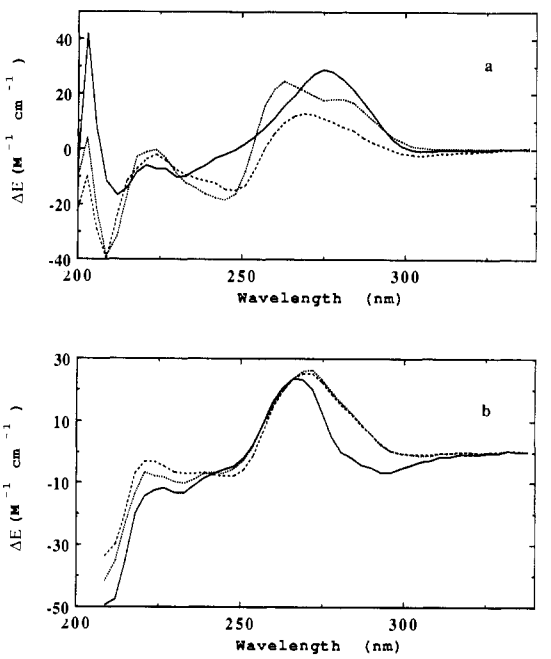

FIGURE 3: Circular dichroism spectra for (a) 1.8×10^{-4} M CGCCGC (—), 9.6×10^{-5} M GCGAGCG (···), and 1.1×10^{-4} M GCGAAGCG (- - -) and for (b) 6.0×10^{-5} M GCGGCG + CGCCGC (—), 6.0×10^{-5} M GCGAGCG + CGCCGC (···), and 9.1×10^{-5} M GCGAAGCG + CGCCGC (- - -). Solutions are 1 M NaCl, 0.01 M sodium phosphate, and 0.1 mM EDTA, pH 7 at 20 °C.

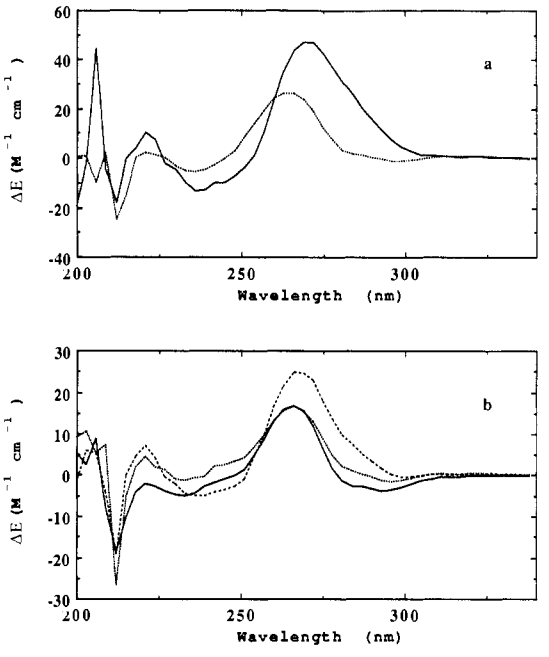

FIGURE 4: Circular dichroism spectra for (a) 9.0×10^{-5} M CGCAACGCA (—) and 9.4×10^{-6} M GCGGCGA (···) and for (b) 9.1×10^{-6} M GCGGCGA + CGCCGCA (—), 5.2×10^{-6} M GCGGCGA + CGCACGCA (···), and 6.7×10^{-6} M GCGGCGA + CGCAACGCA (- - -). Solutions are 1 M NaCl, 0.01 M sodium cacodylate, and 0.5 mM EDTA, pH 7 at 20 °C.

270 nm is broader at longer wavelengths for the bulged duplexes than for the perfect duplexes. The duplexes of CGCCGC with GCGAGCG and GCGAAGCG have similar CD spectra at 20 °C and also at 0 °C (see the supplementary material). This suggests similar overall geometries. The spectra for the individual strands GCGAGCG and GCGAAGCG are unusual (see Figure 3), suggesting their homoduplexes have unusual geometries. GCGAGCG has a positive peak and GCGAAGCG a positive shoulder at about 280 nm that are absent in the other spectra. If $(GCGAGCG)_2$

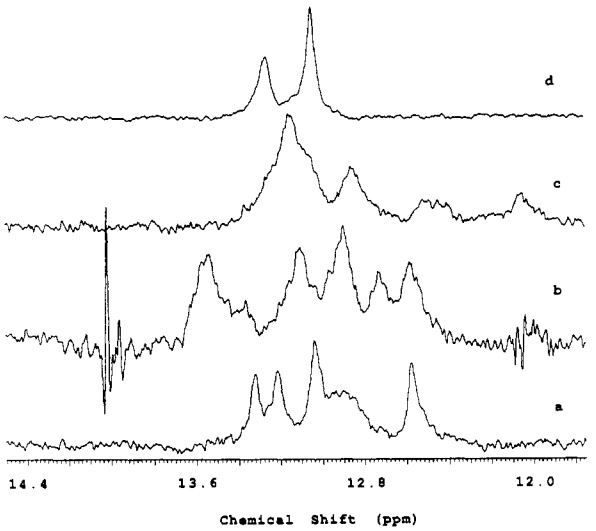

FIGURE 5: NMR spectra of the imino proton region for (a) GCGGCG + CGCCGC, (b) GCGAGCG + CGCCGC, (c) GCGAAGCG + CGCCGC, and (d) GCGAAGCG in 1 M NaCl, 0.01 M sodium phosphate, 0.1 mM EDTA, pH 7 in 10% D_2O/90% H_2O at 0 °C. Oligomer concentration is 2.5×10^{-4} M per strand for duplexes and 7.0×10^{-4} M for GCGAAGCG. Free induction decays of 15424 points were collected and transformed (1.3 Hz/point). A $1:\bar{3}:3:\bar{1}$ pulse sequence (Hore, 1983) was used to suppress the water resonance, and the frequency offset was set to maximize the signal to noise ratio at 12.5 ppm. A 5-Hz exponential line broadening was applied to smooth the spectra.

were present at significant concentrations in mixtures with CGCCGC, then the 280-nm peak would be apparent as a shoulder in CD spectra of the mixture. It is not apparent, indicating $(GCGAGCG)_2$ is not present in significant concentrations. The 280-nm shoulder for $(GCGAAGCG)_2$ is not prominent enough for a similar comparison.

NMR Spectra. Figure 5 presents NMR spectra of imino protons at 0 °C for GCGAAGCG and for equimolar combinations of CGCCGC with GCGGCG, GCGAGCG, and GCGAAGCG. The number of resonances observed and the areas under them provide insight into the number of base pairs formed. For CGCCGC + GCGGCG, five resonance peaks are observed. The peaks at 12.58, 13.22, and 13.32 ppm have approximately equal areas (1.0:0.9:0.9). The area under the overlapping peaks at 12.9 and 13.04 ppm is 3.2 times the area under the peak at 12.58 ppm. This is consistent with formation of the expected six base pairs. For CGCCGC + GCGAGCG, six resonance peaks are observed (12.58, 12.73, 12.90, 13.10, 13.36, and 13.53 ppm), also consistent with formation of six base pairs. For CGCCGC + GCGAAGCG, resonance peaks are observed at 12.05, 12.47, 12.86, and 13.14 ppm with relative areas of 0.5:0.5:1.0:3.2. Some of the area of the 13.14 ppm resonance may come from a small amount of $(GCGAAGCG)_2$. The shoulders of this peak correspond to peak positions observed in the imino proton spectrum of GCGAAGCG (see Figure 5). As shown in Figure 2, the thermodynamic parameters predict about 10% of the strands will form $(GCGAAGCG)_2$ at 0 °C at the 5×10^{-4} M strand concentration of the NMR experiment. Even with this correction, however, the spectrum for CGCCGC + GCGAAGCG seems consistent with formation of six base pairs, if the two resonances with areas of 0.5 are exchanging with water. Such exchange is expected since the T_M for this duplex is 33 °C at 5×10^{-4} M total strands (Kearns et al., 1971). The imino proton spectra are broad and difficult to integrate. Nevertheless, the spectra are consistent with six base pairs forming in all three cases of heteroduplexes. Moreover, there is no clear indication of large concentrations of homoduplexes.

In contrast to the heteroduplexes, the imino proton spectrum for GCGAAGCG has only two resonances, suggesting formation of two different base pairs. This is consistent with formation of the homoduplex $^{GCGAAGCG}_{GCGAAGCG}$.

NMR spectra were also measured for the nonexchangeable base protons at 20 °C for CGCCGC, GCGGCG, GCGAGCG, GCGAAGCG, and duplexes formed by the latter three with CGCCGC when mixed in equimolar proportions [see the supplementary material and Longfellow (1989)]. If significant concentrations of homoduplex were present, then peaks from the homoduplex would be observed in spectra of the mixtures. They are not observed with GCGAGCG + CGCCGC, indicating the heteroduplex is the primary species in solution. The spectrum for GCGAAGCG + CGCCGC is very broad, consistent with either a large number of different species or one species with many alternate conformations.

Discussion

The thermodynamics of bulge loops in RNA is important for prediction of RNA secondary structure. Previous studies characterized bulges in RNA polymers and hairpin stems (Fresco & Lomant, 1975; Fink & Crothers, 1972; Groebe & Uhlenbeck, 1989; Yuan et al., 1979). This is the first study of the thermodynamics of bulges in oligoribonucleotide duplexes.

As discussed under Results, several problems were encountered in this study. A surprising number of non-self-complementary strands form homoduplexes. This can affect thermodynamic parameters if these homoduplexes are present in mixtures designed to form bulged duplexes. Thermodynamic parameters in Tables I and II, however, predict negligible concentrations of homoduplexes, except for GCGAAGCG + CGCCGC. Thermodynamic parameters measured for this case, however, fit patterns established by the other oligomers. Thus we assume thermodynamic parameters for all mixtures reflect primarily the heteroduplex of interest.

Another problem is that most species studied did not melt in a two-state manner. This means $\Delta H°$ and $\Delta S°$ values, and therefore temperature extrapolations, must be treated cautiously. The most certain thermodynamic parameter derived from optical melting is $\Delta G°$ at T_M (Freier et al., 1984). The most useful parameter for prediction of RNA structure is $\Delta G°$ at 37 °C. Fortunately, the longest extrapolations to 37 °C involve duplexes that melt in a two-state manner, GCGGCG + CGCCGC and GCGGCGA + CGCCGCA. Relatively short extrapolations to 37 °C are required for most other sequences. Furthermore, comparison of values in Table II derived from curve fits and from T_M^{-1} plots suggests compensating errors in $\Delta H°$ and $\Delta S°$ lead to reliable values for $\Delta G°_{37}$. Thus we focus on free energy increments for bulge loops at 37 °C. These are calculated as $\Delta G°_{37}$(bulge) = $\Delta G°_{37}$(duplex with bulge) − $\Delta G°_{37}$(duplex without bulge). They are listed in Table IV.

Sequence Dependence of Free Energy Increments for Bulges. All bulges studied destabilize the duplex. The amount of destabilization, however, is sequence dependent. Four aspects of sequence dependence were studied: (1) bulge sequence, (2) nucleotides adjacent to the bulge, (3) sequence not adjacent to the bulge, and (4) bulge size. Each is discussed below.

Bulge Loops of A_n and U_n Have Similar Free Energy Increments. Bulged nucleotides, B, of A and U were studied in the series $GCGB_nGCG$ + CGCCGC. Inspection of Table IV indicates free energy increments were the same within ex-

Table IV: Thermodynamic Parameters for Bulged Loops[a]

oligomer	bulge size	$\Delta G°_{37}$(bulge) (kcal/mol) T_M^{-1} vs log (C_T/4)	$\Delta G°_{37}$(bulge) (kcal/mol) av of fits
GCGAGCG + CGCCGC	1	3.5	3.5
GCGUGCG + CGCCGC	1	3.7	3.5
GCGGCG + CGCACGC	1	3.5	3.6
GCGAGCGA + CGCCGCA	1	5.1	5.4
GCGGCGA + CGCACGCA	1	5.9	5.5
GCAACGA + CGUAUGCU	1	4.6	3.9
GACCGCA + GCGAGUCA	1	2.0	1.3
GCGAAGCG + CGCCGC	2	5.2	5.2
GCGUUGCG + CGCCGC	2	5.4	5.2
GCGGCG + CGCAACGC	2	5.0	4.2
GCGAAGCGA + CGCCGCA	2	7.9	7.2
GCGGCGA + CGCAACGCA	2	7.5	7.0
GACCGCA + GCGAAGUCA	2	5.5	3.8
GCGAAAGCG + CGCCGC	3	5.7	6.0
GCGUUUGCG + CGCCGC	3	5.6	5.7
GCGGCG + CGCAAACGC	3	3.7	3.7
GCGAAAGCGA + CGCCGCA	3	9.2	8.7
GCGGCGA + CGCAAACGCA	3	7.3	6.7
GACCGCA + GCGAAAGUCA	3	7.1	4.3

[a] Parameters are derived from $\Delta G°_{37}$(bulge) = $\Delta G°_{37}$(duplex with bulge) − $\Delta G°_{37}$(duplex without bulge).

perimental error for A_n and U_n bulges. Groebe and Uhlenbeck (1989) reported thermodynamic parameters for two hairpin stem–loops in which the stem contains either a single bulged A or U in the sequence C^{B}C. Melting temperatures with the bulged A and U are 78.6 and 80.0 °C, respectively, consistent with a small effect of sequence in the bulge on stability. Their values of $\Delta G°_{37}$(bulge) are 3.3 and 2.7 kcal/mol, respectively, for the bulged A and U. These are similar to values reported in Table IV in the absence of unpaired terminal nucleotides.

Bulge Loops of A_3 Are More Favorable When Flanked by CGC Than by GCG. For the duplexes GCGGCG + CGCCGC and GCGGCGA + CGCCGCA, bulge loops of A_n were inserted between both of the central GG and CC nearest neighbors. For loops with n = 1 or 2, loop free energy increments were similar on both sides of the helix. The A_3 loop, however, was more unfavorable by about 2 kcal/mol when placed between GG instead of between CC. Papanicolaou et al. (1984) suggested bulge loops between purines might be more stable than those between pyrimidines, on the basis of parameters that gave good computer predictions of secondary structures for tRNA and 5S RNA. This preference is not seen in our results.

Non-Nearest-Neighbor Interactions Affect Free Energy Increments for Bulges. Algorithms for prediction of RNA secondary structure generally assume the free energy increment for a bulge loop depends only on the length of the loop and on the adjacent base pairs. Results in Table IV indicate this is an oversimplification. For example, bulges in the GCGA$_n$GCGA series consistently destabilize the duplex at least 2 kcal/mol more than those in the GCGA$_n$GUCA series. Thus, changing two base pairs not adjacent to the bulge makes a substantial difference. Furthermore, helixes with terminal unpaired nucleotides (dangling ends) are destabilized more by bulges than are helixes without dangling ends. The nearest-neighbor model predicts helixes with and without dangling ends should be equally destabilized. This effect increases with the size of the bulge. For example, GCGGCGA + CGCCGCA is destabilized more than GCGGCG + CGCCGC by about 2 and 3 kcal/mol, respectively, for bulge loops of one and three nucleotides. The results indicate a nearest-neighbor model is not adequate for approximating the effects of bulges on stability. Non-nearest-neighbor effects have also been observed for effects of bulges on the binding of ethidium to RNA (White & Draper, 1987).

Table V: Free Energy Increments for Dangling Ends[a]

oligomer	$\Delta G°_{37}$(d.e.) (kcal/mol) T_M^{-1} vs log (C_T/4)	$\Delta G°_{37}$(d.e.) (kcal/mol) av of fits
GCGGCGA + CGCCGCA	−4.2	−3.6
GCGAGCGA + CGCCGCA	−2.6	−1.7
GCGGCGA + CGCACGCA	−1.8	−1.7
GCGAAGCGA + CGCCGCA	−1.5	−1.6
GCGGCGA + CGCAACGCA	−1.7	−0.8
GCGAAAGCGA + CGCCGCA	−0.7	−0.9
GCGGCGA + CGCAAACGCA	−0.7	−0.7

[a] Parameters were derived from $\Delta G°_{37}$(dangling ends) = $\Delta G°_{37}$(duplex with dangling ends) − $\Delta G°_{37}$(duplex without dangling ends).

It has been suggested that free energy increments for dangling ends may help predict three-dimensional structures of RNA (Sugimoto et al., 1987a,b; Turner et al., 1987, 1988). In particular, strong dangling end stacking is associated with helix extension in tRNA, and weak dangling end stacking is often associated with backbone turns in tRNA. Results in Table II indicate the presence of a bulge may make free energy increments for dangling ends less favorable. These free energy increments are calculated by $\Delta G°_{37}$(dangling ends) = $\Delta G°_{37}$(duplex with dangling ends) − $\Delta G°_{37}$(duplex without dangling ends). These increments are listed in Table V. Helix stabilization from the two dangling ends decreases from −4.2 to −0.7 kcal/mol as bulge size increases from 0 to 3. This suggests a bulge could promote a turn at the end of a helix by weakening dangling end stacking.

Longer Bulges Do Not Always Destabilize More Than Shorter Bulges. It is usually assumed that destabilization due to a bulge increases monotonically as bulge length increases (DeLisi & Crothers, 1971; Gralla & Crothers, 1973). This is true for most sequences listed in Table IV. A_3 bulges in the sequence CA$_3$C, however, are more stable than A_2 bulges in CA$_2$C. This is true for both the CGCA$_n$CGC and CGCA$_n$CGCA series.

Stabilities of Duplexes Formed by Self-Association of Non-Self-Complementary Sequences. Thirteen of the non-self-complementary strands used in this work self-associate to form homoduplexes. These sequences are listed in Table I along with measured and predicted $\Delta G°_{37}$'s for duplex formation. Seven of the measured $\Delta G°_{37}$'s are within 1 kcal/mol of the value predicted from available thermodynamic parameters (Freier et al., 1986; Turner et al., 1988). CGCCGCA and CGCACGCA form duplexes that are more than 1.5 kcal/mol less stable than expected. Four sequences form duplexes that are at least 1.6 kcal/mol more stable than predicted. All four can form internal GA mismatches. GA mismatches are also overrepresented at the ends of helixes and at the beginnings of internal loops in the phylogenetically determined structures for 5S, 16S, and 23S rRNA. If each GA mismatch contributed equally to the difference between measured and predicted stabilities, then each would be more stable than expected by 1 kcal/mol. CD spectra for two of the unusually stable homoduplexes, GCGAGCG and GCGAAGCG, show an unusual peak or shoulder at about 280 nm (see Figure 3). This suggests an unusual conformation. Clearly, sequence dependence of stability and structure for internal loops requires further investigation.

ACKNOWLEDGMENTS

We thank John A. Jaeger for writing the fitting programs for melts of non-self-complementary duplexes and of single strands. We also thank Scott Dreiker for performing some

of the single-strand melting experiments.

Supplementary Material Available

Two tables listing thermodynamic parameters for unimolecular single-strand melting in 1 M NaCl (Table A) and observed and predicted chemical shifts at 70 °C (Table B) and 14 figures showing normalized absorbance vs temperature curves (Figures A, C, and D), T_M^{-1} vs log C_T plots for oligomers (Figures B and E–J), NMR spectra (Figures K and L), and CD spectra of oligomers at 0 °C (Figures M and N) (16 pages). Ordering information is given on any current masthead page.

References

Applequist, J. (1963) *J. Chem. Phys. 38*, 934–941.

Applequist, J., & Damle, V. (1966) *J. Am. Chem. Soc. 88*, 3895–3900.

Brahms, J., Michelson, A. M., & Van Holde, K. E. (1966) *J. Mol. Biol. 15*, 467–488.

Climie, S. C., & Friesen, J. D. (1987) *J. Mol. Biol. 198*, 371–381.

DeLisi, C., & Crothers, D. M. (1971) *Proc. Natl. Acad. Sci. U.S.A. 68*, 2682–2685.

Dewey, T. G., & Turner, D. H. (1979) *Biochemistry 18*, 5757–5762.

Erdmann, V. A., & Wolters, J. (1986) *Nucleic Acids Res. 14*, r1–r72.

Fink, T. R., & Crothers, D. M. (1972) *J. Mol. Biol. 66*, 1–12.

Fink, T. R., & Krakauer, H. (1975) *Biopolymers 14*, 433–436.

Freier, S. M., Hill, K. O., Dewey, T. G., Marky, L. A., Breslauer, K. J., & Turner, D. H. (1981) *Biochemistry 20*, 1419–1426.

Freier, S. M., Albergo, D. D., & Turner, D. H. (1983) *Biopolymers 22*, 1107–1131.

Freier, S. M., Petersheim, M., Hickey, D. R., & Turner, D. H. (1984) *J. Biomol. Struct. Dyn. 1*, 1229–1242.

Freier, S. M., Kierzek, R., Jaeger, J. A., Sugimoto, N., Caruthers, M. H., Neilson, T., & Turner, D. H. (1986) *Proc. Natl. Acad. Sci. U.S.A. 83*, 9373–9377.

Fresco, A. J., & Lomant, J. R. (1975) *Prog. Nucleic Acid Res. Mol. Biol. 15*, 185–218.

Gralla, J., & Crothers, D. M. (1973) *J. Mol. Biol. 78*, 301–319.

Groebe, D. R., & Uhlenbeck, O. C. (1989) *Biochemistry 28*, 742–747.

Gutell, R. R., & Fox, G. E. (1988) *Nucleic Acids Res. 16*, r175–r270.

Gutell, R. R., Weiser, B. Woese, C. R., & Noller, H. F. (1985) *Prog. Nucleic Acid Res. Mol. Biol. 32*, 155–216.

Hader, P. A., Alkema, D., Bell, R. A., & Neilson, T. (1982) *J. Chem. Soc., Chem. Commun.*, 10–12.

Hore, P. J. (1983) *J. Magn. Reson. 55*, 283–300.

Kearns, D. R., Patel, D. J., & Shulman, R. G. (1971) *Nature (London) 229*, 338–339.

Kierzek, R., Caruthers, M. H., Longfellow, C. E. Swinton, D., Turner, D. H., & Freier, S. M. (1986) *Biochemistry 25*, 7840–7846.

Lee, C.-H., & Tinoco, I., Jr. (1980) *Biophys. Chem. 11*, 283–294.

Leng, M., & Felsenfeld, G. (1966) *J. Mol. Biol. 15*, 455–466.

Longfellow, C. E. (1989) Ph.D. Thesis, University of Rochester.

Michel, F., & Dujon, B. (1983) *EMBO J. 2*, 33–38.

Michel, F., & Jacquier, A. (1987) *Cold Spring Harbor Symp. Quant. Biol. 52*, 201–212.

Noller, H. F. (1984) *Annu. Rev. Biochem. 53*, 119–162.

Papanicolaou, C., Gouy, M., & Ninio, J. (1984) *Nucleic Acids Res. 12*, 31–44.

Parker, R., Siliciana, P. G., & Guthrie, C. (1987) *Cell 49*, 229–239.

Peattie, D. A., Doutwaite, S., Garrett, R. A., & Noller, H. F. (1981) *Proc. Natl. Acad. Sci. U.S.A. 78*, 7331–7335.

Petersheim, M., & Turner, D. H. (1983) *Biochemistry 22*, 256–263.

Pörschke, D. (1973) *Eur. J. Biochem. 39*, 117.

Richards, E. G. (1975) *Handbook of Biochemistry and Molecular Biology: Nucleic Acids*, 3rd ed., Vol. 1, p 597, CRC Press, Boca Raton, FL.

Romaniuk, P. J., Lowary, P., Wu, H.-N., Stormo, G., & Uhlenbeck, O. C. (1987) *Biochemistry 26*, 1563–1568.

Schmelzer, C., & Schweyen, R. J. (1987) *Cell 46*, 557–565.

Stannard, B. S., & Felsenfeld, G. (1975) *Biopolymers 14*, 299–307.

Sugimoto, N., Kierzek, R., & Turner, D. H. (1987a) *Biochemistry 26*, 4554–4558.

Sugimoto, N., Kierzek, R., & Turner, D. H. (1987b) *Biochemistry 26*, 4559–4562.

Swokowski, E. W. (1983) *Calculus with Analytical Geometry*, 10th ed., p 139, PWS Publishers, Boston.

Tinoco, I., Jr., Borer, P. N., Dengler, B., Levine, M. D., Uhlenbeck, O. C., Crothers, D. M., & Gralla, J. (1973) *Nature (London), New Biol. 246*, 40–41.

Tunis-Schneider, M. J. B., & Maestre, M. F. (1970) *J. Mol. Biol. 52*, 521–541.

Turner, D. H., Sugimoto, N., Jaeger, J. A., Longfellow, C. E., Freier, S. M., & Kierzek, R. (1987) *Cold Spring Harbor Symp. Quant. Biol. 52*, 123–133.

White, S. A., & Draper, D. E. (1987) *Nucleic Acids Res. 15*, 4049–4064.

Woodson, S. A., & Crothers, D. M. (1987) *Biochemistry 26*, 904–912.

Yuan, R. C., Steitz, J. A., Moore, P. B., & Crothers, D. M. (1979) *Nucleic Acids Res. 7*, 2399–2418.

Zimm, B. H., & Bragg, J. K. (1959) *J. Chem. Phys. 31*, 526–535.

Zuker, M. (1989) *Science 244*, 48–52.

Zuker, M., & Stiegler, P. (1981) *Nucleic Acids Res. 9*, 133–148.